

Investigation of photoaggregation of proteins irradiated by XeCl laser light

L. V. Soustov^a, E. V. Chelnokov^{a*}, N. M. Bityurin^a, V. V. Nemov^b, T. A. Yahno^a,
Yu. V. Sergeev^c, M. A. Ostrovsky^d

^a Institute of Applied Physics Russian Academy of Science, 603600, Nizhny Novgorod, Russia

^b Institute of Epidemiology and Microbiology, 603600, Nizhny Novgorod, Russia

^c National Eye Institute of National Institutes of Health, MD 20892-1860, Bethesda, USA

^d Institute of Biochemical Physics Russian Academy of Science, 117997, Moscow, Russia

ABSTRACT

The effect of XeCl laser radiation on carbonic anhydrase solution is studied. It is investigated that kinetics of protein aggregation is strongly influenced by both laser fluence and repetition rate. The theoretical model is constructed which allows one to explain qualitatively the features of experimental findings.

Keywords: alpha-, beta-, gamma-crystalline, carbonic anhydrase, aggregation, UV laser, fluence, repetition rate

1. INTRODUCTION

Recently there have been many papers reporting on studies of the effect of UV radiation on crystallins, the main structural and functional proteins of vertebral eye lens. This interest has been inspired by the opinion that the effect of UV radiation is one of the most important natural factors of cataract development. The key point in the molecular mechanism for the development of some kinds of cataract is structural destruction of alpha-, beta- and gamma-crystallins [1-4], whose molecular weights are $M_m \sim 800$ kDa, (45-200) kDa and (20-25) kDa, respectively. Under light damage covalent links may appear between amino acid residues of these proteins (further we will call this effect "crosslinking"). This, in turn, leads to the formation of high molecular weight aggregates which are highly scattering and cause lens opaque. These photoaggregation processes are typical for irradiation by mild UV light, whereas in a shorter wavelength range processes of photolysis prevail. This, in particular, was demonstrated in paper [5] where an egg white was irradiated by laser light with wavelengths of $\lambda = 308$ nm and $\lambda = 266$ nm. In experiments on protein photoaggregation either xenon lamp radiation transmitted through a water filter and monochromator adjusted at transmission at $\lambda = 295$ nm, or XeCl laser radiation with $\lambda = 308$ nm are typically used [6, 7]. Absorption of proteins at $\lambda = 308$ nm is one order of magnitude lower than at 295 nm; however, the efficiency of laser irradiation is two orders of magnitude higher due to a higher intensity of laser light. In paper [7] the effect of XeCl laser light on alpha-, beta-, and gamma-crystallins was studied. To register changes occurring in these proteins during irradiation process, kinetics curves were plotted: UV dose D vs intensity of radiation of a test beam scattered in a cuvette with dissolved protein and transmitted through a diaphragm ($D = w \times F \times t$, where w – fluence of the irradiating pulse, F – pulse repetition rate, t – time of irradiation). Beta- and gamma-crystalline solutions became turbid at $D = (500-750)$ J/cm², and scattering of radiation in beta-crystallin began to grow at $D^* \sim 250$ J/cm². In paper [6] the same technique was used to study the effect of radiation at $\lambda = 295$ nm and $\lambda = 308$ nm on different proteins, including carbonic anhydrase solution.

In the literature the UV irradiation was performed at fixed intensity w and at constant repetition rate of light pulses F . The aim of this paper is to study the effect of UV radiation on protein within a wide range of changing of w and F . The object in this study was carbonic anhydrase. We have chosen this protein for the following reasons. Firstly, it is a monomer with molecular weight of 29 kDa. This molecular weight is close to that of gamma-crystallin and some forms of beta-crystallin. Secondly, the behavior of its kinetics curve under XeCl laser irradiation [6] is close to analogous dependences of other proteins, including gamma- and beta-crystallins [7]. In addition to optical methods, we used the high-efficient liquid chromatography method and qualitative analysis of morphology of crystal structures formed at drying a droplet of protein solution [8-10]. Changes in the crystal structure in this case appeared already at $D \sim 1$ J/cm².

* Correspondence: E-mail: che@ufp.appl.sci-nnov.ru; Telephone: +7-8312-384330; Fax: +7-8312-363792

Based on the results of these studies, a physical model of the process of crosslinking formation inside and between protein molecules is developed, and some characteristic parameters of this process are determined.

2. MATERIALS AND METHODS

A physiological phosphate-buffered carbonic anhydrase solution at pH = 7,2 and protein concentration of 0,5 mg/ml was transmitted through a membrane filter with pore sizes of 0,45 μm (Sartorius). Prior to UV irradiation, a vial with protein was kept one hour at room temperature and then was centrifuged during 15 minutes at acceleration of 80 g. A source of UV radiation was a XeCl laser LPX-200 (Lambda Physik) with energy per pulse up to 450 mJ and pulse repetition rate up to 80 Hz. A test beam was from a single-mode (TEM_0) HeNe laser ($\lambda = 633 \text{ nm}$) with power of 10 MW and beam divergence of $1,1 \times 10^{-3} \text{ rad}$. The optical scheme differed from those used in Refs. [6,7] and is illustrated in Fig. 1.

Power of scattered radiation of the test beam was measured by the dark field method [11]. The test beam passing through a quartz cuvette (cuvette dimensions: length along the test beam is 9 mm, along UV beam – 5 mm, and height is 9 mm) with non-irradiated protein solution, was focused by a lens 8 onto a non-transparent screen 9. Since in the process of UV irradiation the appearing scattered radiation led to an increase in test beam divergence, the lens 8 focused this beam in a region behind the screen 9 where a photodiode 10 was placed. Simultaneously with measurements of scattered 633 nm radiation power measurements at a wavelength of 308 nm were performed during UV irradiation. Energy of excimer laser

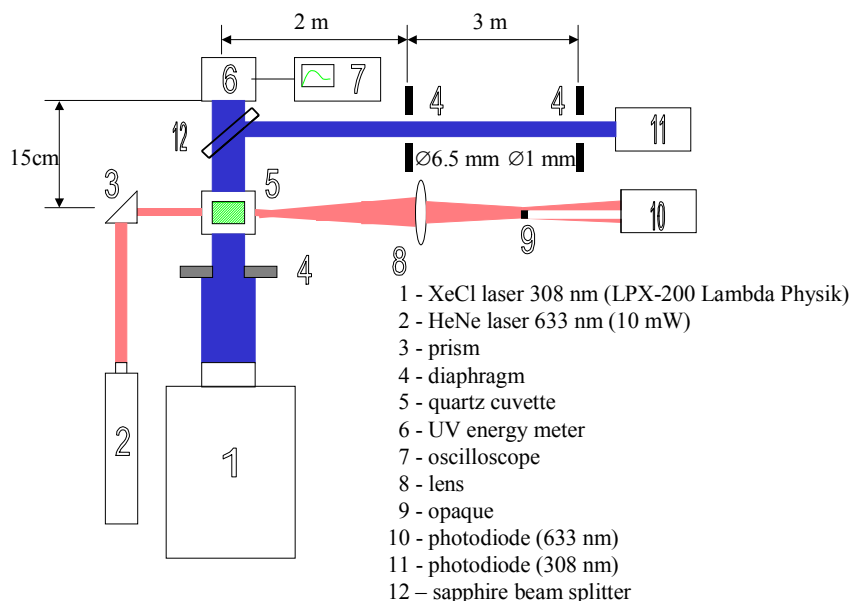


Fig. 1. Experimental scheme.

pulses passed through a protein-containing cuvette was measured by an energy meter Joulemeter ED-200 (Gentec Inc., Canada). The energy meter had an aperture with diameter of 23 mm and was located at a distance of 15 cm after the cuvette. Between the energy meter and cuvette a sapphire plane-parallel plate 0,5 mm in thickness was placed. A 308 nm beam reflected by this plate ($\sim 10\%$ of energy transmitted through the cuvette) passed through a spatial filter. The filter consisted of two diaphragms with diameters of $d_1 = 6,5 \text{ mm}$ and $d_2 = 1 \text{ mm}$, which were separated from each other at a distance $L = 3 \text{ m}$. The radiation attenuated by the spatial filters then went to a UV photodiode LF302UV (Lambda Physik). Using this experimental scheme we measured, immediately in the process of UV irradiation, both the changes in protein absorption at a wavelength of 308 nm and scattering of UV light in the cuvette, which started at irradiation doses one order of magnitude smaller than D^* , the characteristic dose at which scattering of HeNe laser light begins.

After UV irradiation of carbonic anhydrase by different doses, we measured optical transmission spectra by a Carl Zeiss Specord M40 spectrophotometer, and molecular-weight distribution (MWD) using an analytical column for FPLC Superose 12 HR 10/30 (Pharmacia Biotech). Chromatography was performed in buffer: 25 mM, Tris-hcL, 200 mM NaCl, 3 mM NaN_3 (pH = 7,2) with flow speed of 0,3 ml/min. The column was calibrated by molecular-weight standards: blue dextran 2000, thyroglobulin, ferritin, catalase, aldolase, albumin, ovalbumin, chymotrypsinogen, ribonuclease A, cytochrome C, aprotinin, vitamin B_{12} (Pharmacia Biotech, Sigma). Prior to chromatography experiments, samples were filtered through a minimally sorptive filter (PVDF) Millex[®]-GV with pore sizes of 0,22 μm . The effect of small UV doses was registered by a morphological picture of crystallization of a carbonic anhydrase solution droplet, which made it possible to observe the formation of permolecular structures forming specific crystal complexes (dehydration self-organization) [8-10].

3. RESULTS AND DISCUSSION

Before analyzing the kinetics curves, we measured the absorption coefficient α of carbonic anhydrase solution with concentration of 0,5 mg/ml in a cuvette 5 cm in length in the range of XeCl laser radiation intensities $w = (2-300) \text{ mJ/cm}^2$. The value of α was $6 \times 10^{-2} \text{ cm}^{-1}$ and was constant in the whole range of w measurements. This indicates the absence of nonlinear, first of all, two-photon absorption. At such α and at maximal value of $w = 300 \text{ mJ/cm}^2$ used in the experiment heating of protein solution for one pulse was $\Delta T_1 = 1,6 \times 10^{-3}$ degrees Celsius, and heating of the solution during irradiation did not exceed $\Delta T = 2$ degrees Celsius.

The behavior of kinetics curves obtained at different w and F is presented in Fig. 2 a-c. As these figures illustrate, for each w there is a characteristic value of F^* , below which D^* considerably increases (by several times), evidencing a sharp decrease in the probability of crosslinking. At $w = 40 \text{ mJ/cm}^2$ $F^* \sim 6 \text{ Hz}$, at $w = 84 \text{ mJ/cm}^2$ $F^* \sim 2 \text{ Hz}$, and at $w = 300 \text{ mJ/cm}^2$ $F^* \sim 0,3 \text{ Hz}$.

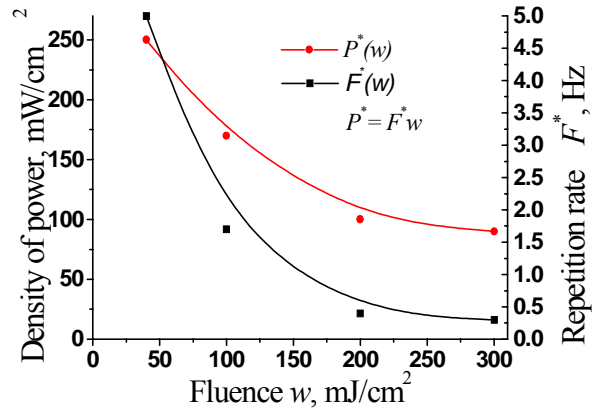
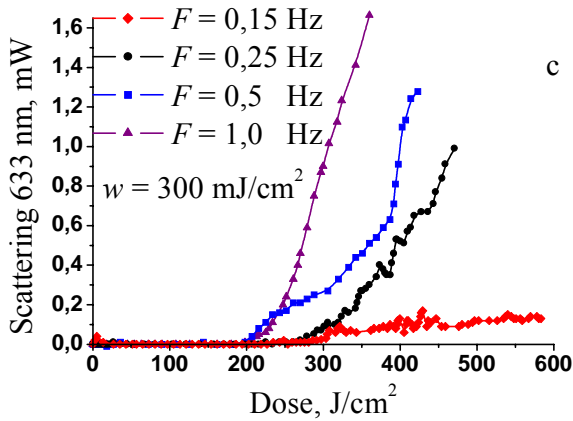
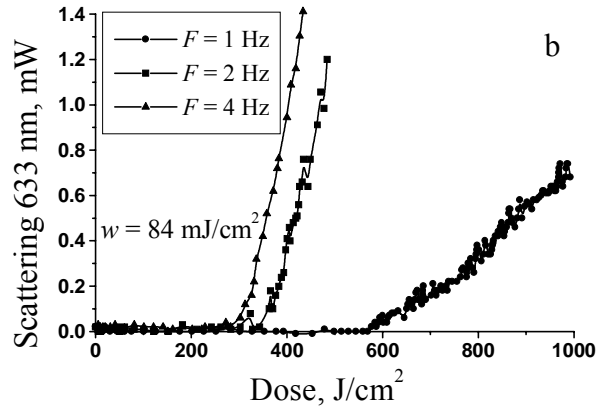
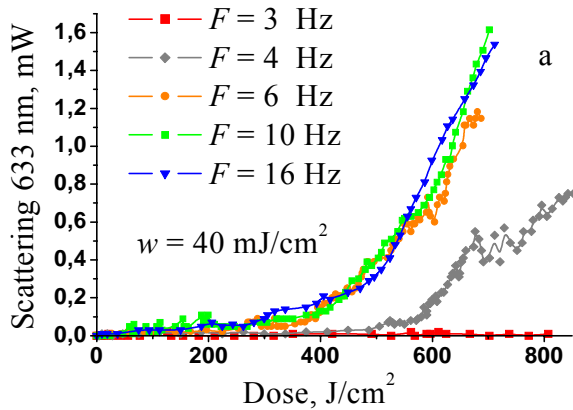


Fig. 2, a-c. Kinetics curves at different fluences and pulse repetition rates

Fig. 3. Power P^* and F^* vs. fluence

Figure 3 presents the dependences of $F^*(w)$ and $p^*(w)$, where $p^* = w \times F^*$, and Figures 4 and 5 – the dependences $D^*(w)$ and $D^*(F)$. It is evident that not only F^* , but also p^* and D^* considerably decrease with increasing w .

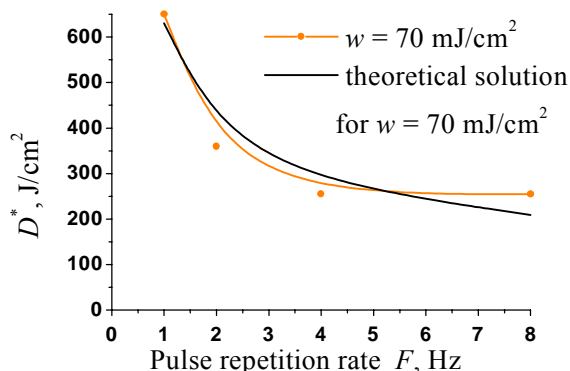


Fig. 4. The dependence of dose $D^*(F)$

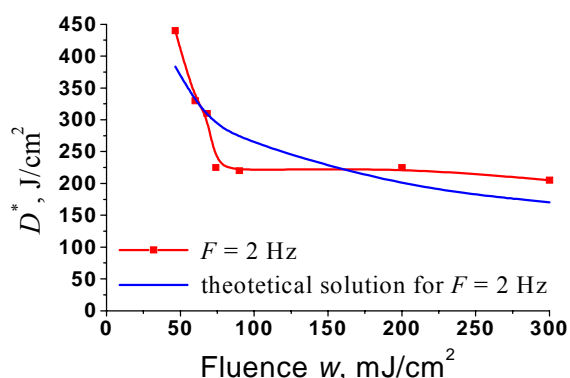


Fig. 5. The dependence of dose $D^*(w)$

Along with the kinetics curve of scattering at 633 nm, Figure 6 shows signals measured by energy meter 6 (curve 1) and UV photodiode 11 (curve 2) vs dose. At small doses, these curves coincide, and starting from $D \sim 20 \text{ J/cm}^2$, the signal from the UV photodiode drops more quickly than from the energy meter. This indicates that at small doses only an increase in absorption of 308 nm radiation in protein solution is recorded in experiment. When the dose is higher, scattering of the UV beam begins to contribute to the signal decrease from the UV photodiode. Since the energy meter is located close to the cuvette, coming scattered radiation does not go beyond aperture of the meter. Therefore, curve 1 is higher than curve 2. Curve 1 characterizes an increase in absorption of 308 nm radiation. Starting from $D \sim 300 \text{ J/cm}^2$ the scattered radiation goes beyond the aperture of the energy meter and the slope of curve 1 increases. Of importance here is the following. The ratio of doses at which scattering of HeNe laser and XeCl laser radiation begins is close to $(633 \text{ nm} / 308 \text{ nm})^4$. Therefore, we can think that at least at the beginning the scattering of radiation with $\lambda = 308 \text{ nm}$ and $\lambda = 633 \text{ nm}$ in protein solution is Rayleigh, i.e., in the both cases the condition $d \ll \lambda$ is obeyed, where d is the size of scattering particles (the radius of a carbonic anhydrase molecule is 2,36 nm [12]).

In protein solutions irradiated by different UV doses at fixed values of $w = 75 \text{ mJ/cm}^2$ and $F = 2 \text{ Hz}$, the molecular weight distributions (MWD) (see Fig. 7) and optical spectra (Fig. 8) were measured. When measuring MWD we evaluated the appearance of different aggregated forms of carbonic anhydrase during irradiation. In the chromatogram of the initial sample, the main fraction of monomer molecules and dimer forms are seen. At $D = 0, 1D^*$ the dimer fraction considerably increases and oligomer forms appear. At $D = D^*$ the dimer and oligomer forms further increase and a fraction of higher molecular weight protein aggregates appears in the region of exclusion limit of the column (from $M_m = 2000 \text{ kDa}$ and more). A dose of $1,5D^*$ leads to the growth of the content of the higher molecular weight protein aggregates, including forms with

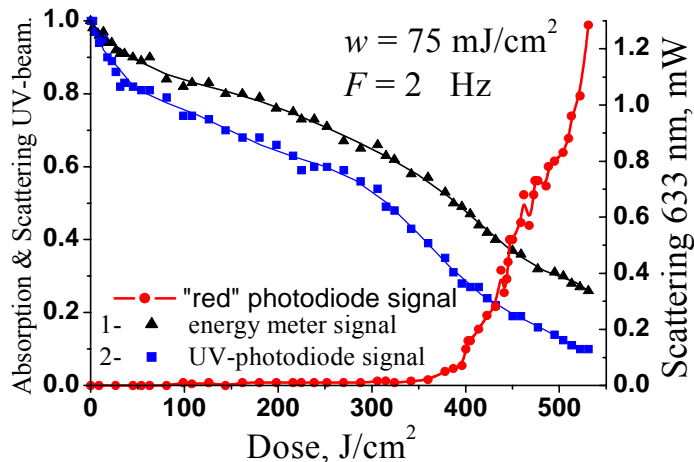


Fig. 6. Kinetics curve of scattering of radiation at 633 nm and curves of absorption and scattering of UV beam

apparent molecular weight more than 2000 kDa (to obtain proportional chromatography profiles different susceptibility was used in measurements of optical density of solution at a wavelength of 280 nm). The comparison of curves in Figs. 2, 6, 7 shows that the growth of scattering of radiation at 308 nm corresponds to the formation of dimer forms in MWD, while the growing scattering of radiation at 633 nm – to the formation of a higher molecular weight protein fraction.

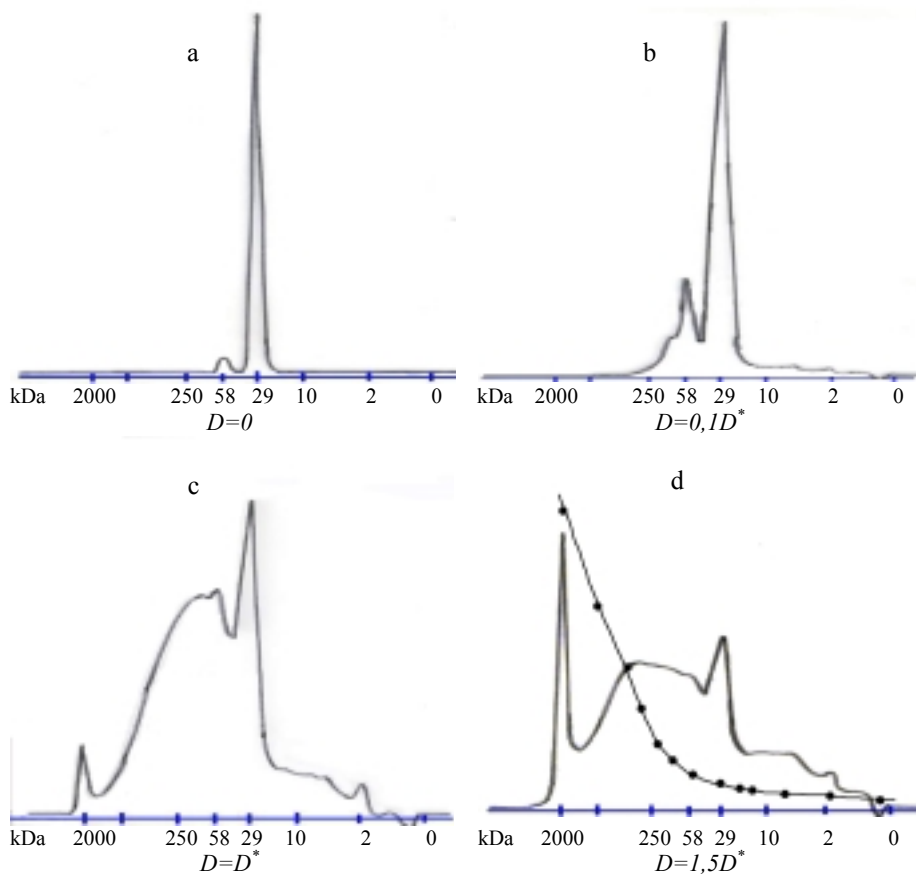


Fig. 7. Molecular weight distributions before (a) and after irradiation at different doses (b,c,d) and calibration curve (d).

Figure 8 shows changes in the optical transmission spectrum of protein at a growing UV irradiation dose. It can be seen that with the increasing dose the transmission monotonically decreases over the whole spectral range measured by us. The same figure demonstrates the spectrum of induced absorption at $D = 1,5D^*$. Its form is analogous to that obtained in Ref. [1] for a UV-irradiated water-soluble fraction of bovine lens. In Fig. 9 changes in the absorption coefficient of carbonic anhydrase solution in the process of UV irradiation at wavelengths of 308 nm and 280 nm are presented. Determining the dependence $\alpha(D)$ for radiation at $\lambda = 308$ nm using a set of spectra (Fig. 8) and by curve 1 in Fig. 6 (a region before its slope starts increasing) yielded similar results.

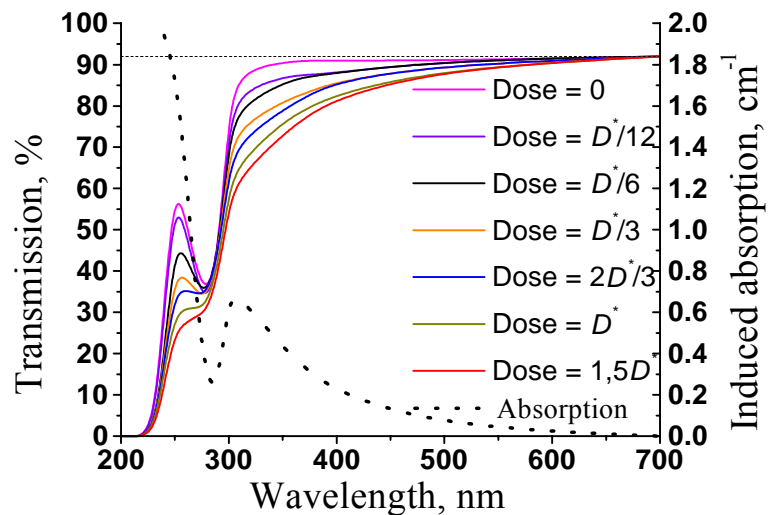


Fig. 8. Optical transmission spectra and spectrum of induced absorption after irradiation with $D = 1,5D^*$

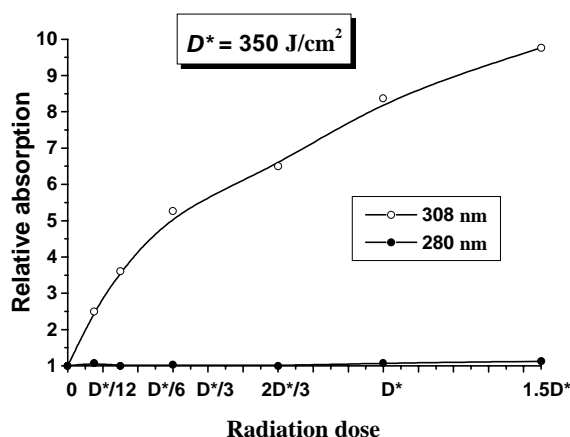


Fig. 9. The dependence of absorption coefficient $\alpha(D)$ of radiation at 308 nm and 280 nm

The effect of small irradiation doses on carbonic anhydrase solution was qualitatively evaluated by changes in the morphology of crystal structures formed at a certain regime of drying of a protein solution droplet on a plane transparent substrate. Photos of typical crystal structures in a central zone of a dried droplet at 70-fold magnification are presented in Fig. 10 a-c. In non-irradiated samples of the carbonic anhydrase solution the central zone of dried droplets is occupied by morphological structures in the form of a circle with a NaCl crystal in the center, which is surrounded by a cascade of concentric laminated crystal formations (Fig. 10 a). After the solution was irradiated by a dose of 1 J/cm^2 , the central-symmetric structural organization of forming structures was destroyed and the laminated crystals are partially replaced by arrow-like crystals (Fig. 10 b). In crystallograms of the solution irradiated by dose of 3 J/cm^2 one can clearly see a further growth of defects of the crystallogram's structural arrangement, consisting in anisomorphy and the replacement of laminated crystals by dendrite-like structures (Fig. 10 c).

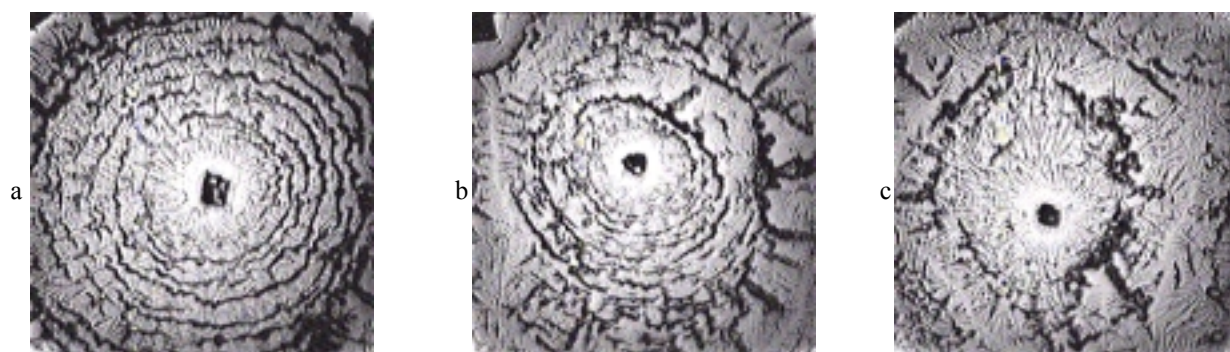


Fig. 10. Crystal structure of a dried solution droplet at 70-fold magnification: a – $D = 0$; b – $D = 1 \text{ J/cm}^2$; c – $D = 3 \text{ J/cm}^2$

Morphology of the crystal structures depends on properties and content of solution. Figure 10 shows changes in the crystallization character under UV irradiation, indicating changes in properties of protein molecules at doses as small as $D \sim 1 \text{ J/cm}^2$. Further studies are needed to make quantitative estimates. However, the results reported here indicate good prospects of using this method for control of photoaggregation processes at early stages of UV irradiation.

4. PHYSICAL MODEL OF PHOTOAGGREGATION

Below we will demonstrate that the experimental results we have obtained can be explained if we assume that aggregation takes place at interaction of two photochemically modified protein molecules. Such a process is analogous to radicals recombination; therefore, further we will refer to the interacting molecules as radicals, though the true nature

of this modification is unclear and requires additional investigations. In addition, in this paper we discuss only the process of dimer formation for we suppose that these are dimers that determine the increase of scattering in protein solution. We will consider three processes here:

- 1) Formation of radicals,
- 2) Their relaxation,
- 3) Aggregation of two radicals with formation of a dimer.

Other processes, including the formation of higher molecular weight protein insoluble aggregates, modification of amino acid residues of tyrosine, tryptophane, and cysteine, are not considered in this model.

Let us write down the equations describing these processes:

$$\begin{aligned}\frac{dR}{dt} &= \mathfrak{R} - kR^2 - \frac{R}{\tau}, \\ \frac{dN}{dt} &= \beta kR^2,\end{aligned}\tag{1}$$

R – concentration of radicals,

N – concentration of dimers,

k – rate constant of the decrease in radical concentration in pair processes,

β – the probability of dimer formation,

τ – characteristic life time of radicals,

\mathfrak{R} – source of radicals.

4.1. CONTINUOUS UV IRRADIATION MODE

In this case the set (1) can be written in the form:

$$\begin{aligned}\frac{dR}{dt} &= \eta\sigma C_0 \frac{I}{\hbar\omega} - kR^2 - \frac{R}{\tau}, \\ \frac{dN}{dt} &= \beta kR^2,\end{aligned}\tag{2}$$

C_0 – concentration of monomer molecules

η – quantum yield of radical formation

σ – effective absorption cross-section

I – radiation intensity

$\hbar\omega$ – photon energy

For a stationary concentration of radicals ($dR/dt = 0$) we find:

$$R = (\sqrt{1 + 4k\tau A} - 1) / 8k\tau,\tag{3}$$

where $A = \eta\sigma C_0 \frac{I}{\hbar\omega} \tau$.

Substituting (3) into (2) yields

$$N(t) = N_0 + t \cdot \beta k (\sqrt{1 + 4k\tau A} - 1)^2 / (8k\tau)^2,\tag{4}$$

where N_0 – dimers concentration that has been accumulated before the stationary level is achieved. If there are no dimers in initial material and the stationary level is quickly achieved $N_0 \sim 0$. Denoting by N^* the dimer concentration at which the growth of scattered radiation is registered, we yield an expression for D^* :

$$D^* = I t^*$$

$$D^* = I \frac{N^*}{\beta k \left(\frac{\sqrt{1 + 4k\tau\eta\sigma C_0 \frac{I}{\hbar\omega} \tau} - 1}{8k\tau} \right)^2},\tag{5}$$

where t^* is the time during which the concentration N^* is accumulated.

In order to simplify the expression (5) let us denote:

$$I_0 = \frac{\hbar\omega}{4k\tau^2\eta\sigma C_0}; \quad D_0 = I_0 \cdot 64N^*(k\tau)^2 / \beta k. \quad (6)$$

Then

$$D^* = D_0 \frac{I/I_0}{\left(\sqrt{1+I/I_0} - 1\right)^2} \quad (7)$$

In limit cases:

$$1) \frac{I}{I_0} \ll 1 \quad D^* = 4D_0 \frac{I_0}{I} \quad (8)$$

$$2) \frac{I}{I_0} \gg 1 \quad D^* = D_0 = \text{const} \quad (9)$$

The total dependence $D^*(I/I_0)$ in dimensionless quantities is given in Fig. 11.

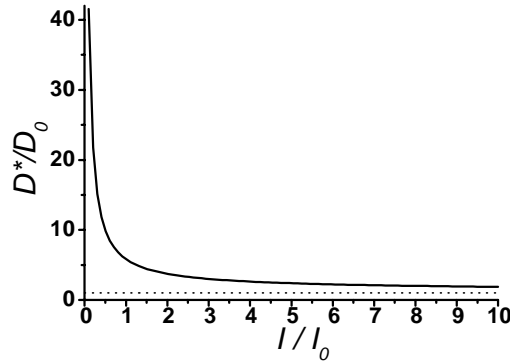


Fig. 11. Dose at the beginning of scattering vs. intensity of continuous UV radiation

Figure 11 shows dose at the beginning of scattering of a test beam of HeNe laser radiation (633 nm) vs. intensity of continuous UV irradiation. This dependence is described by set (2). At small values of I the dependence $D^*(I)$ is a decreasing function of intensity, whereas at high values of I , D^* tends to a constant value D_0 . In this case, the quantity I_0 can be considered to be the boundary between the domain of sharp growth of D^* and the domain where D^* tends to asymptote.

4.2. THE EFFECT OF PULSED UV IRRADIATION ON PROTEIN SOLUTION

In this case the source of radicals is a periodic function of time $\mathfrak{R} = \mathfrak{R}(t-nT)$, where n is an integer. We will solve the set (1) for conditions which have been obeyed in the experiments described above. It can be easily shown that at the concentration of solution used in experiment 10^{16} cm^{-3} (0,5 mg/ml) the time between protein molecules collisions is $\sim 10^{-5} \text{ s}$, which is much greater than laser pulse duration ($3 \times 10^{-8} \text{ s}$). Dimers have too little time to be formed during one laser pulse; therefore in (1) as a source of radicals we can take their concentration R_{0i} , which there is in solution just after a i -th pulse. In this case the set (1) between pulses can be written as:

$$\frac{dR}{dt} = -kR^2 - \frac{R}{\tau} \quad (10)$$

$$\frac{dN}{dt} = \beta k R^2$$

For radical concentration during time between i and $i+1$ pulses we yield:

$$R(t) = \frac{R_{0i}}{\exp(t/\tau) + k\tau R_{0i}(\exp(t/\tau) - 1)}, \quad (11)$$

The concentration after a $(i+1)$ pulse is determined by

$$R_{0(i+1)} = R(T) + R_p,$$

where $R_p = \eta\sigma C_0 \frac{w}{\hbar\omega}$ is an increase in radical concentration after the effect of a pulse with fluence w .

The behavior of dimer concentration is given by an equation obtained from set (10).

$$\frac{dN}{dR} = -\frac{\beta k\tau R}{(1+k\tau R)} \quad (12)$$

The solution of the equation (12) provides a dependence of the increase in dimer concentration during time between i and $(i+1)$ pulses on concentration of radicals:

$$\Delta N(t) = \frac{\beta}{k\tau} \left[k\tau(R_{0i} - R(t)) + \ln \left(\frac{1+k\tau R(t)}{1+k\tau R_{0i}} \right) \right] \quad (13)$$

The dependences $R(t)$ and $N(t)$ are presented qualitatively in Fig. 12 a and b, respectively.

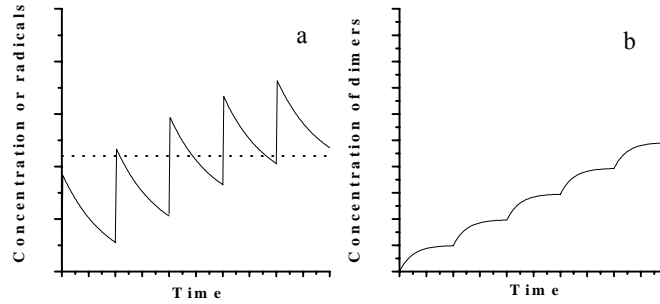


Fig. 12. The growth of concentration of radicals and dimers in the process of pulsed UV irradiation

In the process of radical and dimer formation a stationary regime sets in, when concentration R is saw-tooth and just after a pulse is equal to (R_p+R_s) , while just before the beginning of each subsequent pulse it drops to some constant value R_s . The increase in dimer concentration is equal from pulse to pulse, being:

$$\Delta N(T) = \frac{\beta}{k\tau} \left[k\tau R_p + \ln \left(\frac{1+k\tau R_s}{1+k\tau(R_p+R_s)} \right) \right], \quad (14)$$

$$\text{where } R_s = \frac{R_p}{2} \left(\sqrt{1 + \frac{4}{k\tau R_p (\exp(T/\tau) - 1)}} - 1 \right) \quad (15)$$

The stationary concentration of radicals R_s (15) was obtained from (11) under condition that by the beginning of a next pulse the concentration becomes the same as before the previous pulse. Assuming that scattering begins when dimer concentration reaches some value N^* and knowing the pulse-to-pulse increase of this concentration in the stationary process, we can write down the dose at the beginning of scattering through parameters of pulsed laser radiation and characteristics of the medium:

$$D^* = w \frac{N^*}{\Delta N} = w \frac{N^* k\tau}{\beta} \frac{1}{\left(\chi - \ln \left(1 + \frac{2\chi}{1 - \chi + (\chi+1) \sqrt{1 + \frac{4\chi}{(\chi+1)^2 (\exp(T/\tau) - 1)}}} \right) \right)}, \quad (16)$$

$$\text{where } \chi = k\tau R_p = k\tau \eta\sigma C_0 \frac{w}{\hbar\omega}.$$

Let us introduce some denotations and rewrite equations (16) in the form:

$$D^*(w, F) = D_0 \frac{w/w_0}{(w/w_0 - \ln(1 + \frac{2 \cdot w/w_0}{1 - w/w_0 + (w/w_0 + 1) \sqrt{1 + \frac{4 \cdot w/w_0}{(w/w_0 + 1)^2 (\exp(\frac{1}{F\tau}) - 1)}}))} \quad (17)$$

where $w_0 = \frac{\hbar\omega}{k\tau\eta\sigma C_0}$, $D_0 = w_0 \frac{N^* k\tau}{\beta}$

The expression (17) describes a surface in dimensionless coordinates (dimensionless dose as a function of dimensionless repetition rate of laser pulses and dimensionless fluence) with characteristic scales D_0 , τ and w_0 respectively.

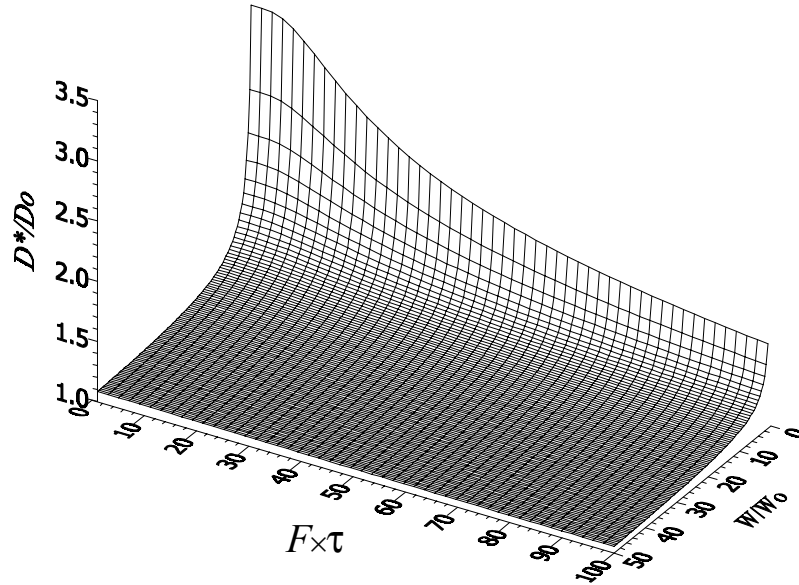


Fig. 13. Dose at the beginning of scattering of a test HeNe laser beam (633 nm) vs. fluence w and repetition rate F

This physical model of aggregation under pulsed UV irradiation describes the dependence of dose at the beginning of scattering of a test HeNe laser beam (633 nm) on characteristics of pulsed radiation: fluence and repetition rate. The three-dimensional dependence given by expression (17) is illustrated in Fig. 13. The section of this surface by a vertical plane parallel to the w/w_0 axis demonstrates the two-dimensional dependence $D^*(w, F = \text{const})$ shown in Fig. 4. At increasing w the value of D^* decreases, tending to a constant level D_0 , while at decreasing w , D^* grows infinitely. This dependence is an analog of the dependence of D^* on intensity of continuous radiation.

Section of this surface by a vertical plane parallel to the $F\tau$ axis shows the dependence $D^*(F, w = \text{const})$ illustrated in Fig. 5. A higher repetition rate corresponds to a lower dose bounded below by the same quantity D_0 as for the dependence $D^*(w)$. A decrease in the repetition rate leads to an increase in D^* . In contrast to the dependence $D^*(w, F = \text{const})$ this growth is bounded above by $D^*_{\max}(w, 0) = 1 / (1 - \ln(1 + w/w_0)^{w_0/w})$.

For better consistency between the theoretical and experimental dependences parameters in equation (17) were fitted. As a result, quantities used in the model were estimated as follows: $D_0 \sim 2 \times 10^2 \text{ J/cm}^2$, $\tau = (10-100) \text{ s}$, $\eta \sim 3 \times 10^{-8}$, $N^*/\beta \sim 10^{12} \text{ cm}^{-3}$. The following experimental values were used for these estimates: $C_0 = 10^{16} \text{ cm}^{-3}$, $\alpha = 6 \times 10^{-2} \text{ cm}^{-1}$, $\sigma = 6 \times 10^{-18} \text{ cm}^2$, $\hbar\omega = 6,62 \cdot 10^{-19} \text{ J}$. It should be underlined that for simplicity the physical photoaggregation model suggested here considered processes of dimer formation only. Other possible processes are not considered, though it is not difficult in principle. This simplified model cannot provide coincidence of experimental and theoretical dependences with high accuracy; however, qualitatively this model can describe the results obtained in experiment.

5. CONCLUSION

A comprehensive study of the effect of XeCl laser radiation on carbonic anhydrase solution is carried out. A strong dependence of the probability of high molecular weight aggregate formation on laser fluence and pulse repetition rate is found. Using the high-efficient liquid chromatography method, the formation of dimers, trimers, oligomers up to polymers with apparent $M_w > 2000$ kDa with increasing UV irradiation dose is demonstrated. Changes in absorption of radiation at 308 nm and scattering of radiation at 308 nm and 633 nm depending on dose are studied. It is shown that at the beginning the scattering of radiation at 308 nm and 633 nm is Rayleigh.

A technique for comprehensive study of the effect of XeCl laser radiation on protein solutions is suggested and used.

A theoretical model is developed, which describes photoaggregation processes occurring in carbonic anhydrase solution under continuous and pulsed UV irradiation. The simplified model which considers only dimer formation not only ensured qualitative coincidence of the theoretical dependence of dose D^* , starting from which scattering of a test beam begins, vs. fluence and repetition rate of UV pulses with experimental curves, but also provided some quantitative estimates.

ACKNOWLEDGEMENTS

This work was financially supported by RFBR grants: № 00-02-16411-a, № 02-04-49342-a, № 02-02-17745-a and RAS Presidium Program “Fundamental science for medicine”. The authors are thankful to S. V. Shubin for his help in carrying out experiments.

REFERENCES

1. M. M. Korhmazyan, I. B. Fedorovich, M. A. Ostrovsky, “Photodamaging mechanism of the eye structure. UV effect on soluble proteins of the lens”. *Biophysics*, **V. 28**, pp. 966-967, 1983.
2. V. V. Elchaninov, I. B. Fedorovich, “Photodamaging mechanism of the eye structure. The aggregates appearance at UV-illumination of soluble lens proteins”. *Biophysics*, **V. 34**, pp. 758-762, 1989.
3. V. V. Elchaninov, I. B. Fedorovich, “Photodamaging mechanism of the eye structure. Change of lens crystalline charges under UV-illumination”. *Biophysics*, **V. 35**, pp. 200-204, 1990.
4. M. A. Ostrovsky, I. B. Fedorovich, V. V. Elchaninov, A. V. Krivandin, “Danger of damaging light action to eye structures. Eye lens – as natural lightfilter and object of photodamaging”. *Sensory Systems*, **V. 8**, № 3-4, pp. 135-146, 1994.
5. N. M. Bityrin, S. V. Muraviov, V. A. Kamensky, A. Yu. Malyshev, E. V. Chelnokov, L. V. Soustov, G. V. Gelikonov, “Kinetics of low scattering biotissue photodenaturation induced by the UV harmonics of a Nd:YAP laser and by Nd:YAG laser at a wavelength of 1440 nm”. *Proc. SPIE*. **V. 4161**, pp. 1-11, 2000.
6. R. F. Borkman, G. Knight, B. Obi, “The molecular chaperone alpha-crystalline inhibits UV-induced protein aggregation”. *Exp. Eye. Res.*, **V. 62**, pp. 141-148, 1996.
7. M. A. Ostrovsky, Yu. V. Sergeev, D. L. Atkinson, L. V. Soustov, J. F. Hejtmancik, “Comparison of UV-induced photo-kinetics for lens-derived and recombinant beta-crystalline”. *Molecular Vision*. **V. 8**, pp. 72-78, 2002.
8. V. N. Shabalin, S. N. Shatohina. *Morphology of biological liquids of human*. 303 p., “Hrisostom”, Moskow, 2001.
9. E. G. Rapis, “Self-organization (self-assembly) of layered protein films”. *Letters to JTPH*. **V. 14**, edition. 17. pp. 1560-1565, 1988.
10. T. A. Yahno, V. G. Yahno, A. G. Sanin, I. I. Shmelev, “Study of the dynamics of phase-transitions in liquids of different types by the method of recording the acoustic-mechanical impedance of a drying-up drop”. *Biophysics (in print)*.
11. E. L. Bubis, V. V. Vargin, L. R. Konchalin, A. A. Shilov, “Investigation of lowabsorptive mediums for SBS in near IR wavelength range”. *Optics and spectroscopy*. **V. 65**, № 6. pp. 1281-1285, 1988.
12. K. P. Wong, C. Tanford, “Denaturation of bovine carbonic anhydrase B by guanidine hydrochloride. A process involving separable sequential conformational transitions”. *J. Biol. Chem.* **V. 248**(24), pp. 8518-8523, 1973.
13. L. V. Soustov, E. V. Chelnokov, N. M. Bityurin, V. V. Nemov, T. A. Yahno, Yu. V. Sergeev, M. A. Ostrovsky. “Investigation of photoaggregation of proteins irradiated by XeCl laser light”. 19 p. Preprint IAP RAS № 599, Nizhny Novgorod, 2002.